

NONLINEAR DYNAMIC ANALYSIS OF REINFORCED CONCRETE FRAMED STRUCTURES INCLUDING SOIL-STRUCTURE INTERACTION EFFECTS

Dr. M. N. Mahmood
Lecturer

S. Y. Ahmed
Assistant Lecturer

Civil Eng. Dept.-Mosul University

ABSTRACT

The role of soil-structure interaction on seismic behavior of reinforced concrete structures is investigated in this paper. Finite element approach has been adopted to model the interaction system, that consists of a reinforced concrete plane frame, soil deposit, and interface which represents the frictional surface between the foundation of the structure and subsoil. The analysis is based on the nonlinear characteristics of the materials and the elasto-plastic behavior of the frame members (beams and columns) is governed by a yield surface which is defined by ultimate strength of the axial force-bending moment interaction, while the cap model is adopted to govern the elasto-plastic behavior of the soil material. Results deduced from the dynamic analysis indicate that soil-structure interaction can have beneficial effects on structural behavior and this behavior is dependent on the characteristics of the soil and the interface conditions.

KEY WORDS

earthquake, force-bending interaction diagram, interface, reinforced concrete, soil-structure interaction

INTRODUCTION

The dynamic soil-structure interaction has long been a topic of interest in engineering practice. This problem has a considerable influence on the response of massive structures such as dams, bridges and multi-story frames. For these reasons, the development of appropriate methods for the analysis is increasingly demanded to ensure the integrity of structural design.

In general, the structure including its foundation will interact with the soil, and analyzing the structure isolated from the soil will cause deviating solution. The seismic excitation of the structure and the subsoil may be considered as one of the most severe loading case. The researches in this subject have not yet provided a full understanding of how the soil-structure interaction affects the response of the structure subjected to dynamic loads. Thus a comprehensive study is required to investigate the response of a structure under seismic loading and its sensitivity to various parameters.

Chen and Krauthammer ^[1] used a combined finite element-finite difference method with substructuring approach to solve the soil-structure interaction problems subjected to seismic loading. The study concentrated on the importance of the

mathematical modeling of the interaction system. Phan *et al.* [2] compared the elastic response of 6-story building subjected to an earthquake loading using two different boundary conditions, in the first, the frame is assumed to be fixed at supports, and in the second case the interaction between the structure and the subsoil is considered. The study clarified the effect of considering the soil-structure interaction on the structural response. The soil medium was represented by simple elastic springs. Dunand *et al.*[3] estimated the modal frequencies and damping ratios of 26 reinforced concrete buildings from ambient vibration records. The estimated data were used in the analysis of these buildings taken into consideration the soil-structure interaction. The main emphasis was to determine the damping resulting from the soil layer itself during the interaction analysis and its contribution in absorbing vibrational energy of the structure. Todar *et al.* [4] used a vast amount of earthquake response records of a reinforced concrete multistory frame, constructed over a soil with pre-specified parameters. The study aimed to investigate various aspects that affect the dynamic behavior of the soil-structure system. The main objectives of the present work are to evaluate the sensitivity of plane frame structures to different variables related to soil and interface conditions when the structure is subjected to an earthquake excitation.

MATHEMATICAL FORMULATIONS

Finite element approach has been adopted in the present work to model the interaction system, which consists of three main parts, in particular the structural frame members, soil layers, and the interface between the foundation of the structure and the subsoil. Details of these elements are presented as follows.

Two-Node Beam-Column Element

The members of a reinforced concrete plane frame are idealized by two-node beam-column elements, each node has three degrees of freedom (u, v, θ) and the stress resultants corresponding to these degrees of freedom are axial force, shear force, and bending moment. The elastic stiffness and mass matrices for any two-dimensional beam-column element are derived using the bending theory for small transverse displacements and it is well described in many textbooks of structural mechanics [5].

Four-Node Isoparametric Plane Strain Element

The soil layer, which is considered as an integrated part of the interaction system, is idealized by four-node plane strain elements with two degrees of freedom at each node (u, v) . The stress-strain relation developed in the element can be written in the following form [6]:

$$\begin{Bmatrix} \sigma_x \\ \sigma_y \\ \tau_{xy} \end{Bmatrix} = [D] \begin{Bmatrix} \varepsilon_x \\ \varepsilon_y \\ \gamma_{xy} \end{Bmatrix} \quad \dots (1)$$

where σ_x, σ_y are the normal stresses, τ_{xy} is the shear stress, $\varepsilon_x, \varepsilon_y$, and γ_{xy} are the corresponding strains, and $[D]$ is the elasticity matrix for plane strain condition.

Based on the energy minimization, the elastic stiffness and mass matrices can be determined from the relations:

$$[K] = \int_v [B]^T [D] [B] dv \quad \dots (2)$$

$$[M] = m \int_v [N]^T [N] dv \quad \dots (3)$$

where $[B]$ is the strain-displacement matrix, $[N]$ is the shape function matrix of the element, m is the distributed mass on the element area, and v is the volume of element. The numerical integration of the above equations is carried out using 2×2 Gauss quadrature [6].

Interface Element

The present interface element is formulated to model the interface between the foundation of the structure and the soil elements. The element is assumed to have a unit thickness and degrees of freedom compatible with other two elements. The interface element shown in Figure (1) has two nodes at each end, lower and upper nodes, having the same coordinates. The upper

node adjacent to a frame element has three degrees of freedom (u, v, θ) , while the lower one, adjacent to the soil (plane strain) element, has two degrees of freedom (u, v) . The stress-strain relation of this element can be written in the following form ^[7,8]:

$$\begin{Bmatrix} \tau_s \\ \sigma_n \\ M \end{Bmatrix} = [C] \begin{Bmatrix} \varepsilon_{s_1} \\ \varepsilon_n \\ \varepsilon_{s_2} \end{Bmatrix} \quad \dots (4)$$

where τ_s, σ_n , and M are the shear stress, normal stress, and bending moment at the interface, respectively, $\varepsilon_{s_1}, \varepsilon_n$, and ε_{s_2} are the corresponding strains, and $[C]$ is the constitutive matrix of the interface which can be written as:

$$[C] = \begin{bmatrix} C_{s_1} & 0 & 0 \\ 0 & C_n & 0 \\ 0 & 0 & C_{s_2} \end{bmatrix} \quad \dots (5)$$

in which C_n, C_{s_1} , and C_{s_2} are uncoupled normal, shear, and rotational stiffnesses of the interface, respectively. For the isoparametric interface element, the displacements and rotation at any point on the element are interpolated from nodal values as follows:

$$u = \sum_{i=1}^2 N_i u_i \quad , \quad v = \sum_{i=1}^2 N_i v_i \quad , \quad \text{and} \quad \theta = \sum_{i=1}^2 N_i \theta_i \quad \dots (6)$$

where N_i is the shape function which is defined for node i of one dimensional element by using natural coordinates r , which varies from (-1) for node 1 to $(+1)$ for node 2 as:

$$N_i = (1 + rr_i)/2 \quad \dots (7)$$

where r_i is the natural coordinate of node i .

The strain vector in global coordinates at any point of the element can be expressed in terms of the nodal values of the relative displacements at the nodes as:

$$\begin{Bmatrix} \varepsilon_{s1} \\ \varepsilon_n \\ \varepsilon_{s2} \end{Bmatrix} = \frac{1}{t} \sum_{i=1}^2 \begin{bmatrix} N_i & 0 & 0 \\ 0 & N_i & 0 \\ 0 & 0 & N_i \end{bmatrix} \begin{Bmatrix} \Delta u_i \\ \Delta v_i \\ \Delta \theta_i \end{Bmatrix} \quad \dots (8)$$

or

$$\{\varepsilon\} = \frac{1}{t} \sum_{i=1}^2 [B]_i \{\Delta\} \quad \dots (9)$$

where t is the thickness of the element which is taken equal to unity, and $(\Delta u_i, \Delta v_i, \text{ and } \Delta \theta_i)$ are the relative displacements between the upper and lower nodes which are equal to:

$$\{\Delta_i\}^T = \{u_1^t - u_1^b, v_1^t - v_1^b, \theta_1^t, u_2^t - u_2^b, v_2^t - v_2^b, \theta_2^t\} \quad \dots (10)$$

where superscripts t and b correspond to the top and bottom nodes, respectively. The elastic stiffness matrix of this element can be derived by the following formula:

$$[K] = \int_v [B]_i^T [C] [B]_i dv \quad \dots (11)$$

where $[B]_i$ represents the strain-displacement matrix, and v is the volume of element.

MATERIAL MODELING

Reinforced Concrete Material

The material model adopted for reinforced concrete frame members is represented by the interaction diagram between the ultimate axial load p_u and the bending moment m_u , where this interaction diagram represents the yield surface for two-dimensional analysis of the reinforced concrete sections.

The development of axial load-bending moment interaction curve for any reinforced concrete section (beam or column) requires (i) stress-strain relations for plain concrete and reinforcing steel, and (ii) dimensions of the section and the amount and locations of reinforcement. The uniaxial stress-strain relation as proposed by Medland and Taylor^[9] shown in Figure (2a) has been adopted to model the behavior of concrete in compression. While Figure (2b) shows the idealized stress-strain relation used to model the reinforcing steel behavior.

To determine the axial load-bending moment interaction curve for a rectangular reinforced concrete section shown in Figure (3), the section is assumed to be subjected to a normalized axial load P and moment m . The non-dimensional equilibrium

equations of force and moment (about neutral axis) at any stage of loading are:

$$p = \frac{1}{\phi} \int_{\varepsilon_c} \frac{\sigma_c}{f_c'} d\varepsilon_c + \sum_{i=1}^n \frac{A_{si}}{bd} \frac{\sigma_{si}}{f_c'} bdf_c' \quad \dots (12a)$$

$$m = \frac{I}{\phi^2} \int_{\varepsilon_c} \frac{\sigma_c}{f_c'} d\varepsilon_c + \frac{I}{\phi} \sum_{i=1}^n \frac{A_{si}}{bd} \frac{\sigma_{si}}{f_c'} \varepsilon_{si} - P \left(\frac{\varepsilon_t}{\phi} - 0.5 \right) d \quad \dots (12b)$$

where ϕ is a curvature at the section, f_c' is compressive strength of concrete, and the other remaining symbols in Equation (12) are defined in Figure (3). Applying the adopted stress-strain relations of the plain concrete and the reinforcing steel shown in Figure (2) will simplify the equilibrium Equation (12) for the next calculations.

Assuming ε_t equal to the ultimate concrete strain in compression ε_u , and substituting different values of curvature ϕ (by varying the neutral axis depth), a set of points (p_u, m_u) is obtained by using Equation (12). A third degree polynomial is then fitted to the calculated set of points (p_u, m_u) by using the least squares method. This polynomial may be expressed as:

$$\frac{m_u}{m_o} = a_1 + a_2 \left[\frac{p_u}{p_o} \right] + a_3 \left[\frac{p_u}{p_o} \right]^2 + a_4 \left[\frac{p_u}{p_o} \right]^3 \quad \dots (13)$$

where m_o is the ultimate bending moment of the section in the absence of axial load, p_o is the ultimate axial load of the section

in the absence of bending moment, and $(a_1, a_2, a_3, \text{ and } a_4)$ are constants of the polynomial. Equation (13) can be used in calculating the interaction diagram for any reinforced concrete section during the analysis. Then the yield function of any section can be defined as:

$$\left| \frac{m}{m_u} \right| = 1.0 \quad \dots (14)$$

in which m is the current normalized bending moment applied on the section.

Soil Material

The nonlinear elasto-plastic constitutive relationship of soil material that is based on the cap model, originally proposed by DiMaggio ^[10], is adopted in the present study. The cap model shown in Figure (4) consists of two parts: an ultimate failure envelope which limits the maximum shear stresses attainable by the material and elliptically shaped strain-hardening yield surface that produces plastic volumetric and shear strains as it expands. The failure envelope portion is described by Drucker-Prager yield surface for loading and failure ^[11]:

$$h(I_1, \sqrt{J_2}) = \sqrt{J_2} - \alpha I_1 - z - \beta \exp(-\gamma I_1) = 0 \quad \dots (15)$$

where I_1 is the first invariant of the stress tensor, J_2 is the second invariant of the deviatoric stress tensor, β and γ are material

constants which are calculated from the laboratory tests, and α and z are equal to:

$$\alpha = 2 \sin \phi / [\sqrt{3}(3 - \sin \phi)] \quad \dots (16)$$

$$z = 6c' \cos \phi / [\sqrt{3}(3 - \sin \phi)] \quad \dots (17)$$

in which ϕ , and c' are the angle of friction and cohesion of the soil, respectively.

The strain-hardening surface (Elliptical Cap) can be described mathematically by the following Equation ^[1]:

$$H(I_1, \sqrt{J_2}, k) = \sqrt{J_2} - \frac{1}{R} \{ [X(k) - L(k)]^2 - [I_1 - L(k)]^2 \}^{\frac{1}{2}} \quad \dots (18)$$

where R is the ratio of the major to the minor axis of the elliptic cap, $X(k)$ and $L(k)$ depend on the hardening parameter k .

$X(k)$ can be calculated from the relation:

$$X(k) = -\frac{1}{D} \ln(1 - \frac{k}{W}) \quad \dots (19)$$

where D is a material constant which is calculated from the laboratory tests, and W defines the maximum plastic volumetric compaction that the material can experience under hydrostatic loading. Finally, the loading function f can be expressed as follows:

$$f = \begin{cases} h(I_1, \sqrt{J_2}) & \text{if } I_1 \leq L(k) \\ H(I_1, \sqrt{J_2}, k) & \text{if } I_1 > L(k) \end{cases} \quad \dots (20)$$

Interface for Dynamic Soil-Structure Interaction

The response of a soil-structure system subjected to dynamic loading such as those resulting from earthquake and blasts can be influenced by the characteristics of joints (interfaces) between the structure and the soil. Assuming perfect bond at the interface during all stages of loading usually simplifies the analysis procedure significantly. Under dynamic loading, several modes such as sliding, separation or debonding can occur at the interface during vibration of the structure. The interface element is treated essentially like any other solid (soil, or structural) element, but its constitutive relations are defined differently. The constitutive relation matrix $[C]$ of this element, given in Equation (5), consists of normal, shear, and bending stiffness.

High values are assigned for the normal and bending stiffness to avoid interpenetration of neighboring solid elements. Selection of these high values is based on the characteristics of the surrounding materials (structural and geological materials). Therefore, the adopted relation to express the normal and bending stiffness can be written in the following form ^[12]: -

$$[C_{s_2}] = [C_n] = \lambda_1 [C_n]_t + \lambda_2 [C_n]_g + \lambda_3 [C_n]_{st} \quad \dots (21)$$

The subscripts (t), (g) and (st) are corresponding to the interface, geological, and structural materials, respectively, and ($\lambda_1, \lambda_2, \text{ and } \lambda_3$) are the participation factors which may vary from (0) to (1) and can be obtained from appropriate laboratory tests.

The normal stiffness of the interface $[C_n]_t$ is estimated from the following ^[13]:

$$[C_n]_t = \frac{E(1-\nu)}{(1+\nu)(1-2\nu)} \quad \dots (22)$$

where E is the elastic modulus, and ν is Poisson's ratio.

The shear part $[C_s]$ of the interface is equal to the shear modulus G_i that is obtained from the results of direct shear tests of interface shown in Figure (5). The shear modulus G_i is derived from the shear stress of the interface through the following expression:

$$G_i = \frac{\partial \tau}{\partial U_r} \cdot t' \quad \dots (23)$$

where τ is the shear stress at interface, U_r is the relative shear displacement between the top and bottom nodes, and t' is the thickness of interface element.

Using the direct shear test results indicated in Figure (5). It is possible to obtain a polynomial fit of the form:

$$\tau = \alpha_1 + \alpha_2(u_r) + \alpha_3(u_r)^2 \quad \dots (24)$$

in which α_1, α_2 , and α_3 are the interface parameters, that can be expressed as:-

$$\alpha_i = \beta_1 + \beta_2 \cdot (\sigma_n) + \beta_3 \cdot (\sigma_n)^2 + \beta_4 \cdot (N) + \beta_5 \cdot (N)^2 \quad \dots (25)$$

where σ_n is normal stress, and N is number of cycles in direct shear test. The coefficients α_i and β_i associated with the shear behavior of the interface element can be determined from the results of appropriate laboratory tests ^[13].

The shear stress in Figure (5) is steadily increasing for increasing number of cycles, but there is an ultimate shear stress, the level of this stress is determined by a slip function, and can be written in the following expression:

$$F_s = |\tau| - (c_a + \sigma_n \tan \delta) \quad \dots (26)$$

In which c_a is the activated adhesion, and δ is the activated friction angle. Slip occurs at the interface when:

$$\sigma_n + \Delta\sigma_n < 0 \quad (\text{Compressive stresses}) \quad \text{and} \quad F_s > 0 \quad \dots (27)$$

in this case Newton-Raphson iterations are used to adjust the shear stresses (making F_s approaching zero value), and the plastic displacement (slip) at the interface resulting from this adjustment, is determined.

The element goes into separation or debonding mode if:

$$\sigma_n + \Delta\sigma_n \geq 0 \quad (\text{Tensile stresses}) \quad \dots (28)$$

In this case neither normal nor shear traction can be transmitted through the interface and these stress components are set to zero.

Rebonding between the adjacent elements is returned if the normal stresses at the interface become:

$$\sigma_n + \Delta\sigma_n \leq 0 \quad (\text{Compressive stresses}) \quad \dots (29)$$

INELASTIC ANALYSIS

Inelastic Analysis of the Frame Members

In general, the yield condition of the frame members can be expressed as:

$$f = f(p_k) = 1.0 \quad \dots (30)$$

where p_k represents the nodal forces or stress resultants; $f < 1$ implies an elastic state; $f = 1.0$ represents yielding and $f > 1.0$ represents non-admissible state. In classical theory of plasticity, the flow rule states that the plastic deformation rates are linearly related to their corresponding force (or stress) rates ^[14]. The associated flow rule can be written as:

$$\{du_p\} = \lambda \cdot \{g\} \quad \dots (31)$$

in which $\{du_p\}$ is plastic components vector of the incremental nodal displacements, λ is flow constant, and $\{g\}$ is the gradient vector of the yield surface.

In the elastic-perfectly plastic material, there is no secondary plastic work, this implies that the increment of the

nodal forces dp corresponding to a plastic deformation of a particular cross-section must be tangent to the yield surface.

$$du_p^T \cdot dp = 0 \quad \dots (32)$$

By using the above equations, the flow constant can be derived assuming that the incremental nodal displacements of the element are decomposed into elastic and plastic components.

$$du = du_e + du_p \quad \dots (33)$$

The elastic components of displacements will create incremental nodal forces dp :

$$dp = k_e \cdot du_e \quad \dots (34)$$

$$\text{or } dp = k_e \cdot (du - du_p) \quad \dots (35)$$

where k_e is the elastic stiffness matrix of the element. By substituting the value of du_p from Equation (31), the resulting equation is:

$$dp = k_e \cdot du - k_e \cdot g \cdot \lambda \quad \dots (36)$$

By multiplying the two sides of Equation (36) by g^T and using the flow rule and the normality condition referred in Equations (31) and (32) respectively, then:

$$g^T \cdot dp = g^T \cdot k_e \cdot du - g^T \cdot k_e \cdot g \cdot \lambda = 0 \quad \dots (37)$$

Solving for λ , then:

$$\{\lambda\} = [g^T \cdot k_e \cdot g]^{-1} g^T \cdot k_e \cdot du \quad \dots (38)$$

$\lambda \geq 0$ implies loading condition, and $\lambda < 0$ implies elastic unloading condition.

Inelastic Analysis of the Soil

As mentioned in the previous sections, the loading function is assumed to be isotropic and to consist of two parts as specified in Equation (20). The plastic loading criteria for the function f is given by:

$$d\sigma_{ij} \frac{\partial f}{\partial \sigma_{ij}} \begin{cases} > 0 & \text{Loading} \\ = 0 & \text{Neutral loading} \\ < 0 & \text{Unloading} \end{cases} \quad \dots (39)$$

In which σ_{ij} is the stress tensor.

The first step to determine the possible path of the stresses is made by computing the elastic trial stresses σ_{ij}^e and checking the stress path resulting from the strain increment as shown in Figure (6).

NUMERICAL APPLICATION AND DISCUSSION

Description of the Problem

The soil-structure interaction system, shown in Figure (7), is considered for investigating the structural response predicted by the nonlinear dynamic analysis using the developed computer

program of the present study. Details of the cross sections of beams, columns, and foundation of the superstructure are shown in Figure (8). The system is subjected to an earthquake signal shown in Figure (9) at node 61 near the rigid base. In the present study the predicted structural response is presented in terms of horizontal displacement of node 1 (at top of the structure) and the slip between two opposite nodes at the interface (nodes 13 and 18). The properties of the materials used in the analysis are summarized as follows:

◆ Structural properties

Concrete material

Young's modulus, E_c	= 20700	N/mm ²
Poisson's ratio, ν_c	= 0.167	
Density, ρ_c	= 2240	kg/m ³
Compressive strength, f'_c	= 20	N/mm ²

Reinforcing steel

Young's modulus, E_{st}	= 200000	N/mm ²
Yielding strength, f_y	= 400	N/mm ²

◆ Soil properties (Ottawa sand) ^[12]

Young's modulus, E_s	= 26	N/mm ²
Poisson's ratio, ν_s	= 0.370	
Density, ρ_c	= 1700	kg/m ³

◆ Parameters for the cap model ^[12]

$$\beta = 0.20 \text{ N/mm}^2, \quad Z = 0.20 \text{ N/mm}^2, \quad W = 0.00267, \\ R = 2.5, \quad D = 1.20 \text{ 1/(N/mm}^2), \quad \gamma = 2.03 \text{ 1/(N/mm}^2), \\ \alpha = 0.4$$

◆ Properties of the interface

$$\text{Young's modulus, } E_i = 26 \quad \text{N/mm}^2$$

$$\text{Poisson's ratio, } \nu_i = 0.37$$

$$\text{Friction angle, } \tan \delta = 0.576$$

The numerical integration is performed using time step (0.0005 sec), and the damping ratio of the overall system is assumed to be 5% (Rayleigh damping) ^[15].

Dynamic Analysis

The dynamic analysis has been carried out by using the Predictor-Corrector Newmark's algorithm ^[16], to study the structural response to an idealized earthquake signal applied at node 61. Figure (10) shows the response of the structure in terms of horizontal displacement at node 1, the figure shows also comparison between the results predicted from the present analysis with that predicted, for the same system shown in Figure (7), by Haggblad and Nordgren ^[17]. They used the plain concrete as a structural material of the frame members assuming elastic behavior of concrete and elasto-plastic behavior of soil material throughout the analysis. Considerably higher response is obtained for the horizontal displacement of node 1 when the acceleration of the input signal climbs over a certain level.

Figure (11) shows the horizontal response at nodes 13 and 18 at the interface adjacent to the soil surface (at bottom of the foundation of the structure). The difference between the horizontal displacements of these nodes gives an indication about

the amount of slip at the interface near the corner of the foundation.

Figure (12) shows comparison between the structural response at node 1 when slip is permitted at the interface with that for perfect bond between the structure and the soil. This difference in displacement justifies the importance of employing the slip model at the interface points.

Figure (13) shows the significant difference in the response at node 1 for two different models of the soil behavior, in particular elasto-plastic behavior represented by the cap model and linear elastic behavior. The figure shows the dependency of the response of the entire structure on the material model of the soil medium especially during the analysis to earthquake transmitted through this medium.

Figure (14) describes the relative horizontal movement between the interface nodes 13 and 18. The slip is relatively small at the first 2 seconds from the time of excitation, after this time the rate of slip is steadily increased till it reaches a value of 6.5 mm at the time of 3 second.

CONCLUSIONS

A simple interface element that allows for deformation modes, such as no slip, slip, separation, and debonding, is used for simulating the interface behavior between the structure and subsoil elements during the interaction analysis. The study assures the importance of dependency of the structure on the

behavior of soil material, especially in the analysis of the interaction system subjected to an earthquake excitation transmitted through the soil media. Incorporation of slip model in the interface elements significantly affects the behavior of the structure. The experiences from the numerical analysis indicate that the chosen material models, for the soil and for the structure, which are robust for classical engineering work, are sufficiently stable and gave reliable results.

REFERENCES

- 1) Chen, Y., and Krauthammer, T., "A combined adina-finite difference approach with sub-structuring for solving seismically induced nonlinear soil-structure interaction problems ", Computers and Structures, Vol. 32, No. 3/4, pp. 779-785, 1989.
- 2) Phan, L. T., Hendrikson, E. M., Marshall, R. D., and Celebi, M., "Analytical modeling for soil-structure interaction of a 6-story commercial office building", 5th U.S. National Conference on Earthquake Engineering, Vol. 1, 1994.
- 3) Dunand, F., Bard, P. Y., Vassail, T., and Gueguen, P., "Evidence of strong influence of soil-structure interaction for buildings damping ratio from ambient vibration recordings", Proceedings of the 12th European Conference on Earthquake Engineering, paper No. 869, London, 2003.

- 4) Todar, G., Yamazaki, F., and Katayama, T., "Observation and numerical analysis of soil-structure interaction of a reinforced concrete tower ", Journal of Earthquake Engineering and Structural Dynamics, Vol. 24, pp. 491-503, 1995.
- 5) Taueer, F. F., Sacone, E., Fillipo, F. C., "A fiber beam-column element for seismic response analysis of reinforced concrete structures", Report No. UCB/EERC-91/17, Earthquake Engineering Research Center, College of Engineering, University of California, Berkeley, 1991.
- 6) Owen, O. R. J., and Hinton, E., "Finite elements in plasticity, theory and practice", Pineridge press, Swansea, UK, 1980.
- 7) Guclehus, G., "Finite elements in geomechanic ", John-Wiley & Sons, Ltd., 1977.
- 8) Viladkar, M. N., Godbole, P. N., and Noorzai, J., "Modeling of interface for soil-structure interaction studies", Computers and Structures, Vol. 52, No. 4, pp. 565-779, 1994.
- 9) Medland, I. C., and Taylor, D. A., "Flexural rigidity of concrete column section", Journal of Structural Engineering Division, ASCE, Vol. 97, No. ST2, pp. 573-586, 1971.

- 10) DiMaggio, F. L., Sandler, I. S., "Material model for granular soil", Journal of Engineering Mechanics Division, ASCE, Vol. 97, No. EM3, pp. 935-950, 1971.
- 11) Chen, Y., and Krauthammer, T., "A combined adina-finite difference approach with sub-structuring for solving seismically induced nonlinear soil-structure interaction problems ", Computers and Structures, Vol. 32, No. 3/4, pp. 779-785, 1989.
- 12) Desai, C. S., Zamman, M. M., Lighther, J. G., "Thin layer element for interface and joints ", International Journal for Numerical and Analytical Methods in Geomechanics, Vol.8, pp. 19-43, 1984.
- 13) Zamman, M. M., Desai, C. S., Drumm, E. C., "Interface model for dynamic soil-structure interaction ", Journal of Geotechnical Engineering, Vol. 110, No. 9, pp. 1257-1272, September 1989.
- 14) Chen, W. F., "Plasticity in reinforced concrete", McGraw-Hill Inc., New York, 1982.
- 15) Tedesco, J. W., McDougal, W. G., and Ross, C. A., "Structural dynamics: theory and applications", Addison Wesley Longman, Inc., California, USA, 1999.
- 16) Wilson, L. E., "Three dimensional static and dynamic analysis of structures", Computers and Structures Inc., Berkeley, California, USA, 2002.

- 17) Dunand, F., Bard, P. Y., Vassail, T., and Gueguen, P.,
“Evidence of strong influence of soil-structure interaction
for buildings damping ratio from ambient vibration
recordings“, Proceedings of the 12th European Conference
on Earthquake Engineering, paper No. 869, London, 2003.

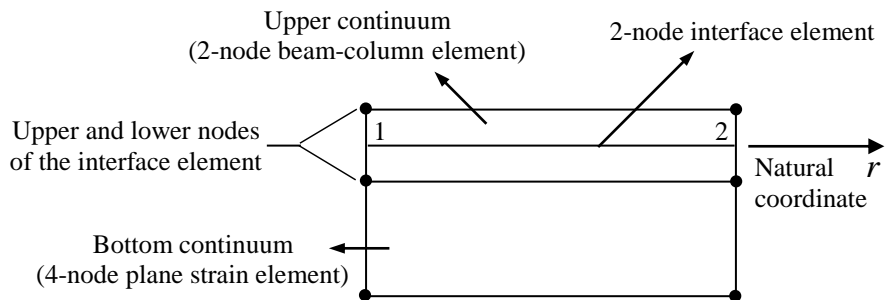
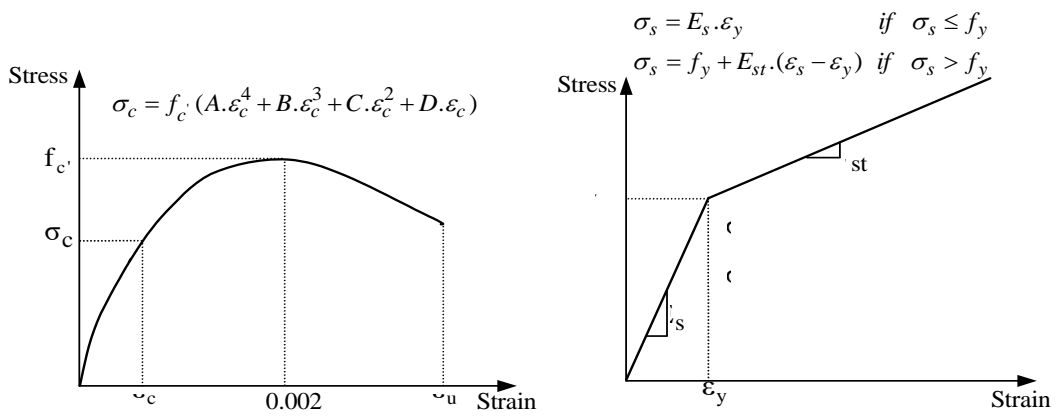


Figure (1) Geometry of 2-node isoparametric interface element



(a) Uniaxial stress-strain relation for concrete

(b) Idealized stress-strain relation for steel

Figure (2) Stress-strain relations of concrete and reinforcing steel

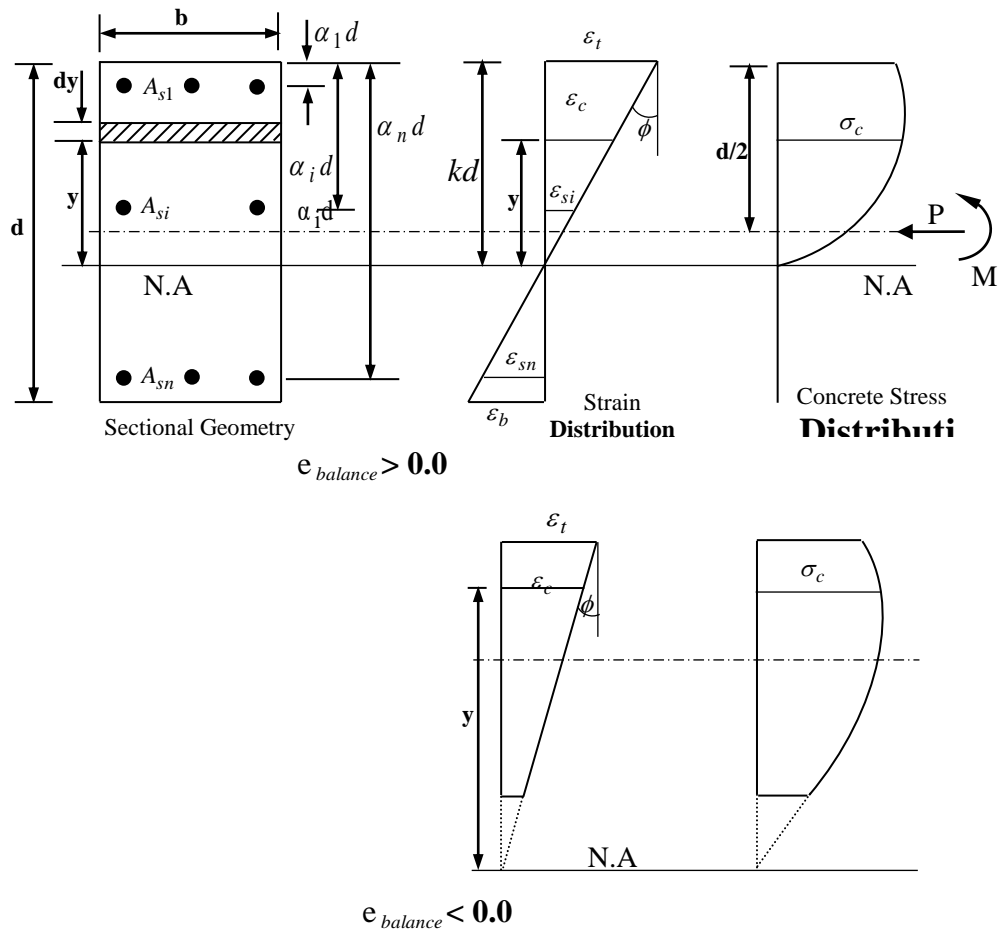


Figure (3) Sectional geometry and possible stress-strain distribution

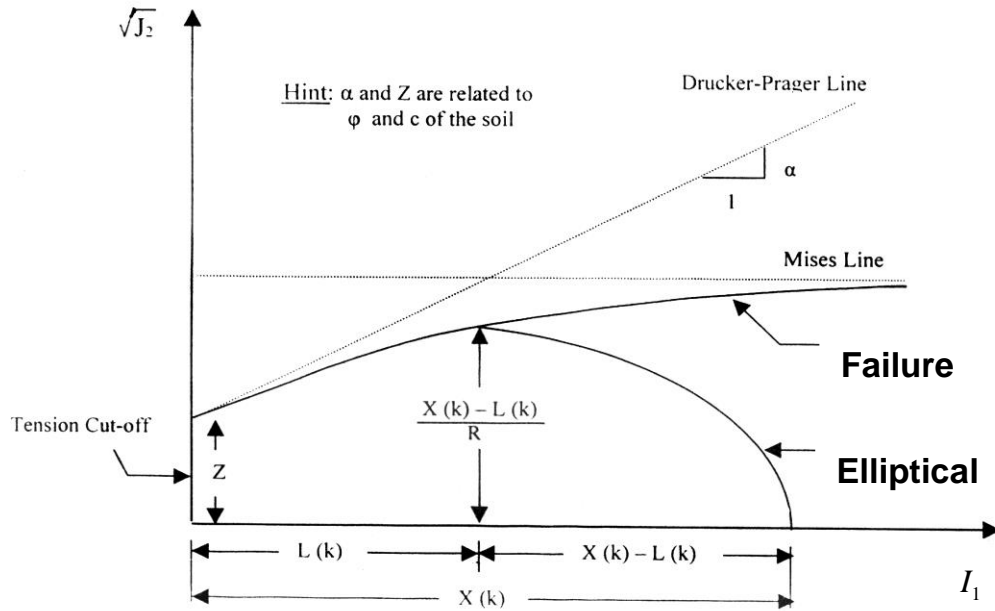


Figure (4) Cap model

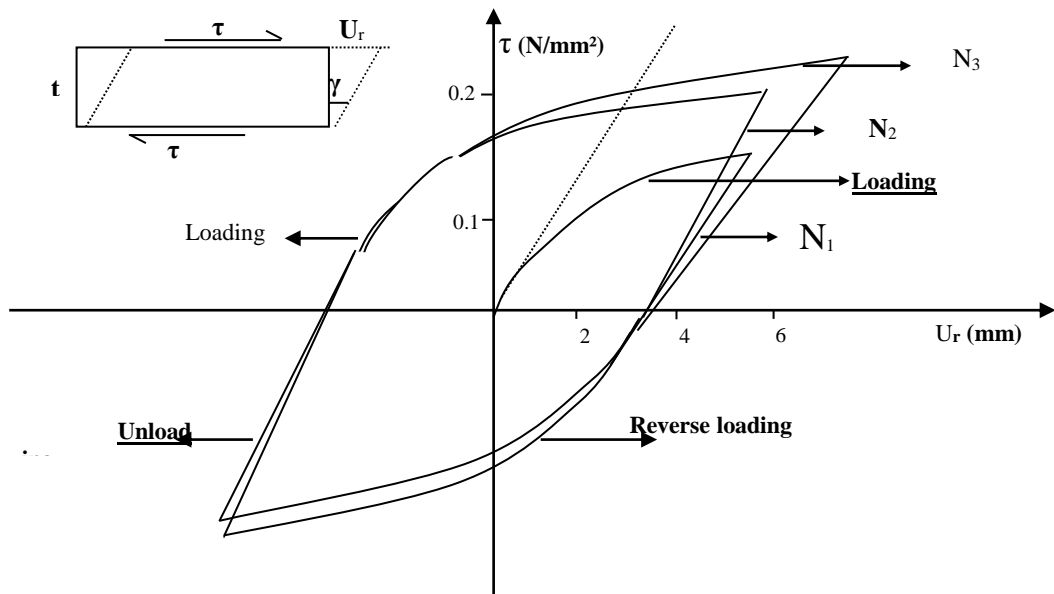


Figure (5) Direct shear test

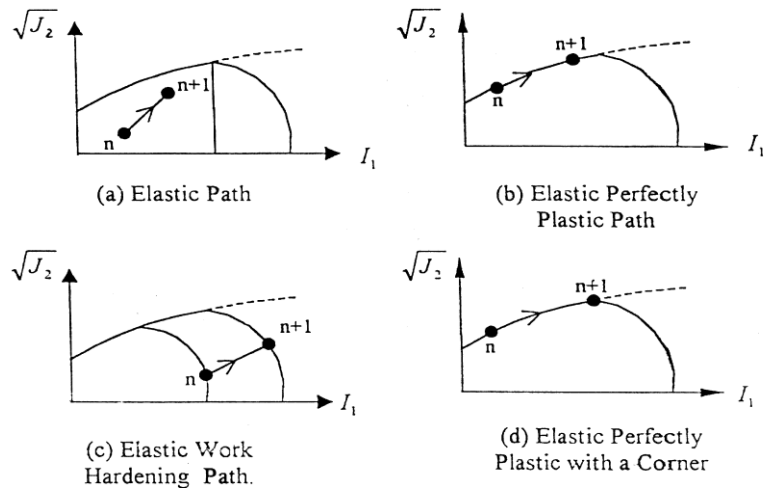


Figure (6) Possible stress paths resulting from a strain increment

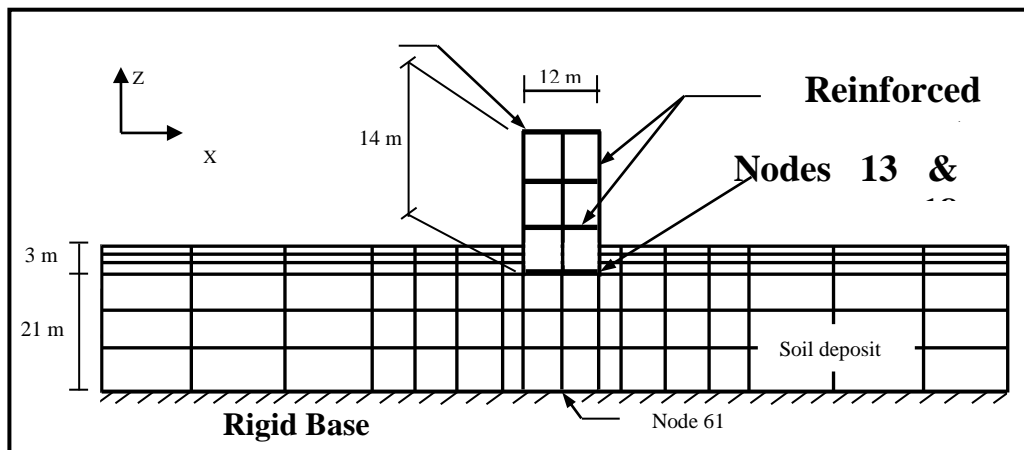


Figure (7) Soil-structure interaction model

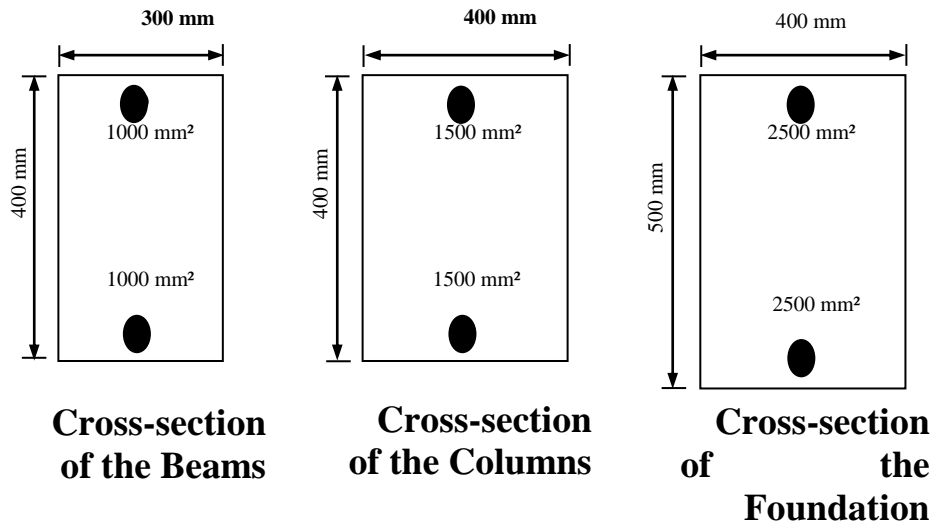


Figure (8) Cross sections of beams, columns, and foundation of the superstructure

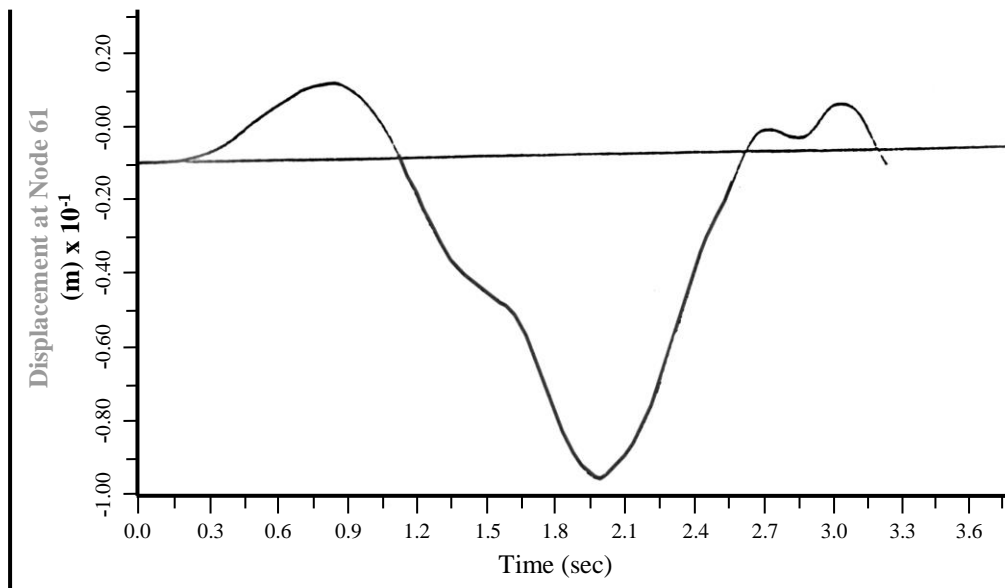


Figure (9) Input signal (prescribed displacement at the base in x-direction)

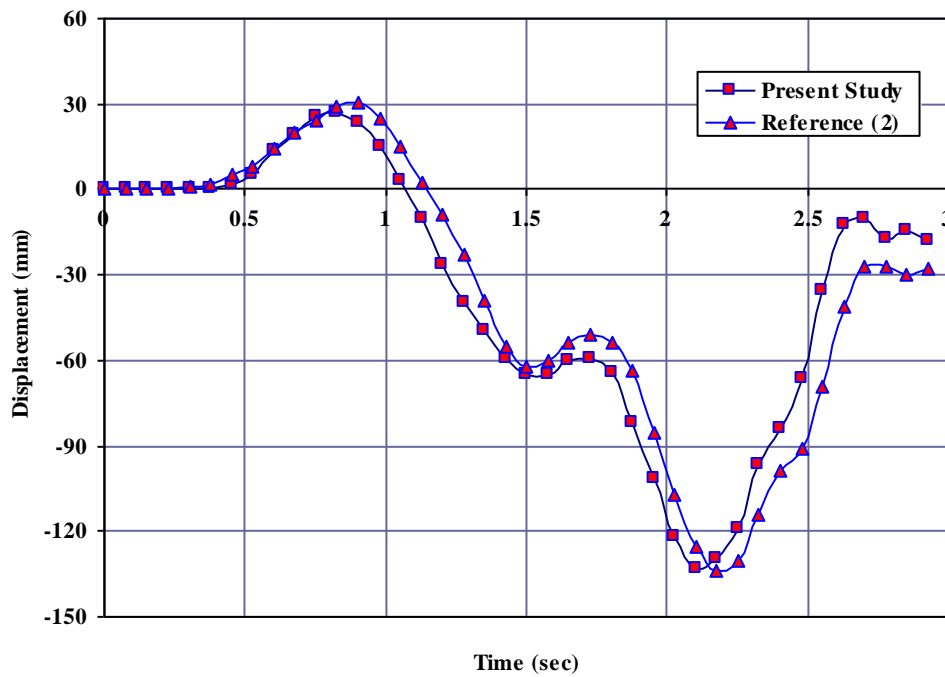


Figure (10) Displacement-time history at node 1 in X-direction.

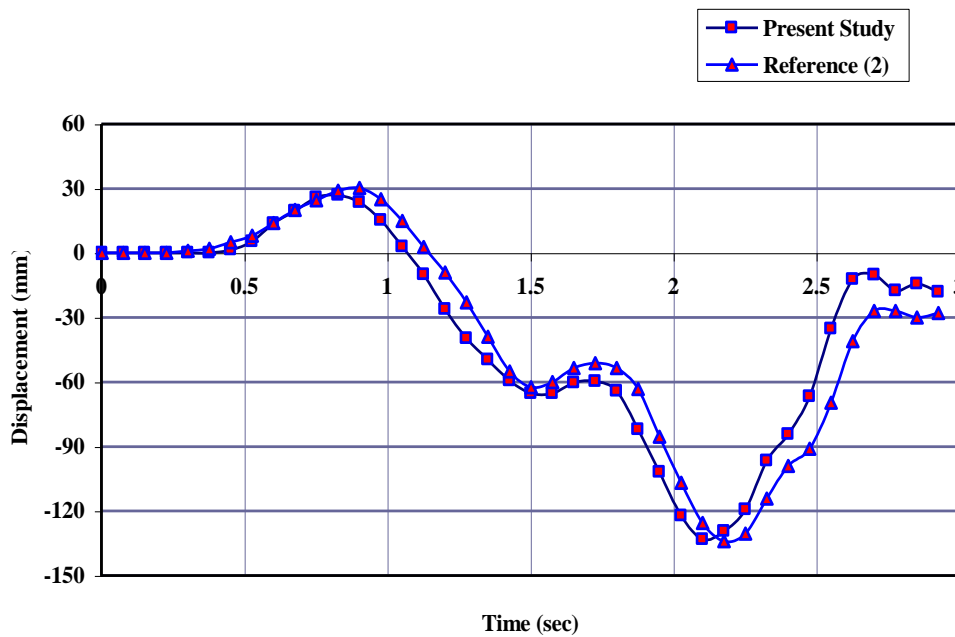


Figure (11) Slip at the interface in X- direction

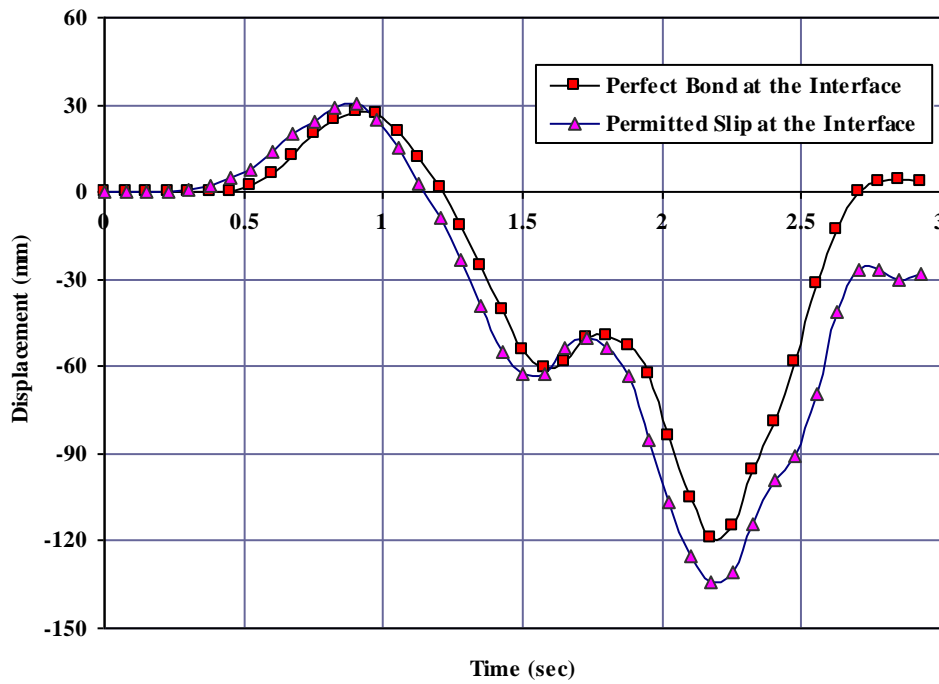


Figure (12) Displacement-time history at node 1 in X- direction different models of the interface

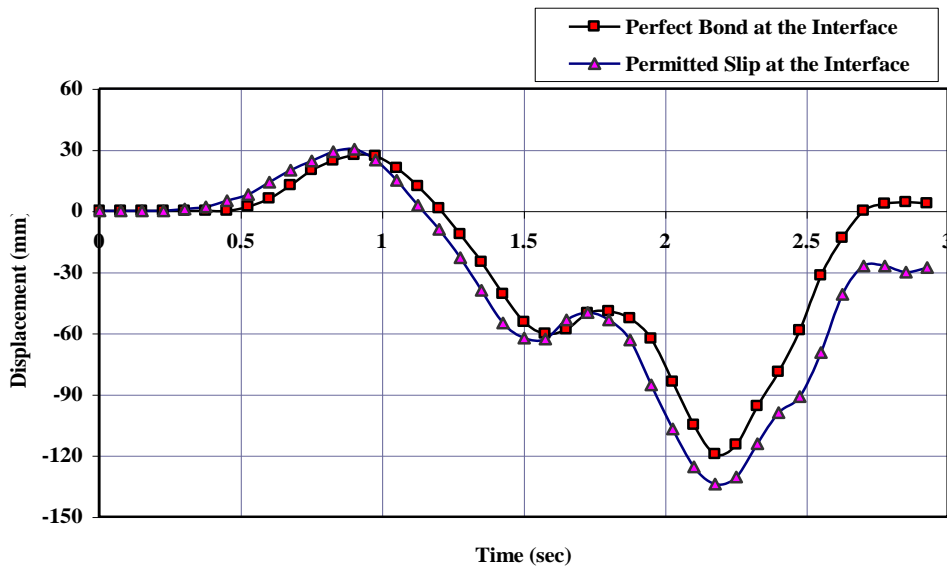


Figure (13) Displacement-time history at node 1 in X- direction different behaviors of soil material

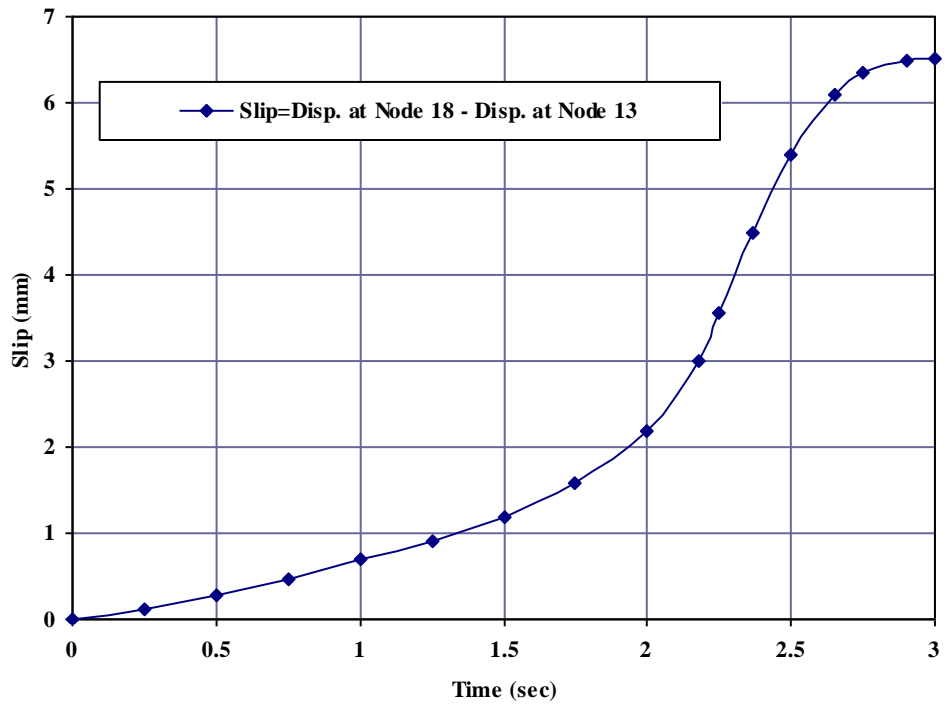


Figure (14) Amount of slip between 18 & 13

التحليل اللاخطي الديناميكي للهياكل الإنشائية الكونكريتية المسلحة مع احتواء تأثيرات تداخل التربة-المنشأ

سفيان يونس احمد

د. محمد نجم محمود

قسم الهندسة المدنية-جامعة الموصل

الخلاصة

يهدف هذا البحث إلى دراسة تأثير تداخل المنشأ مع التربة على التصرف الزلزالي للمنشأ الخرساني المسلح . طريقة العناصر المحددة أختيرت لتمثيل منظومة التداخل والتي تتكون من الهيكل الخرساني المسلح المستوي (ذات البعدين), طبقات التربة, وسطح التداخل الذي يمثل السطح الاحتكاكي بين أساس المنشأ والتربة. التحليل يعتمد على الخواص اللاخطية للمواد والتصرف المرن-اللدن لعناصر الهيكل (الأعمدة والجسور) تحكم بسطح الخضوع المعرف بعلاقة التداخل بين القوة المحورية القصوى وعزم الانحناء الأقصى للمقطع الخرساني المسلح, بينما موديل الغطاء يتم اختياره ليحكم التصرف المرن-اللدن لمادة التربة.النتائج المستحصلة للتحليل الحركي تدل على ان تداخل المنشأ مع التربة يمتلك تأثيرات مفيدة على تصرف المنشأ وهذا التصرف معتمد على خواص مادة التربة وسطح التداخل بين الأساس وسطح التربة

الكلمات الدالة

الهزة الأرضية, مخطط التداخل للقوة-العزم, التلامس, الخرسانة المسلحة, تداخل المنشأ-التربة